NASA TECHNICAL NOTE

NASA TN D-6267

NASA TN D-6267

ANALOG COMPUTER STUDY OF DESIGN PARAMETER EFFECTS ON THE STABILITY OF A DIRECT-ACTING GAS PRESSURE REGULATOR

by Miles O. Dustin

Lewis Research Center
Cleveland, Ohio 44135

NATIONAL AERONAUTICS AND SPACE ADMINISTRATION • WASHINGTON, D. C. • MARCH 1971

1. Report No. NASA TN D-6267	2. Government Accession No.	3. Recipient's
4. Title and Subtitle ANALOG COMPUTER STUDY OF DESIGN PARAMETER EFFECTS ON THE STABILITY OF A DIRECT-ACTING GAS PRESSURE REGULATOR		5. Report Date March 1971 6. Performing Organization Code
7. Author(s) Miles O. Dustin		8. Performing Organization Report No. E-6015
9. Performing Organization Name and Address Lewis Research Center National Aeronautics and Space Administration Cleveland, Ohio 44135		10. Work Unit No. 720-03 11. Contract or Grant No.
12. Sponsoring Agency Name and Address National Aeronautics and Space Administration Washington, D.C. 20546		13. Type of Report and Period Covered Technical Note 14. Sponsoring Agency Code

15. Supplementary Notes

16. Abstract

An analog simulation of a spring-loaded, direct-acting, single-stage gas pressure regulator is presented. The simulation was based on a pressure regulator used in a solar Brayton cycle space power generator. The effects of regulator design parameters on stability, transient response, and steady-state accuracy were examined. Regulator stability was improved by increasing spring rate, decreasing sensing orifice size, and increasing output volume. The effect of adding an orifice in series with the metering poppet valve was also investigated. A comparison was made between the dynamic performance of the simulated regulator and the actual Brayton cycle regulator.

17. Key Words (Suggested by Author(s))

Gas regulator
Pressure regulator
Analog simulation
Analog computer
Automatic control
Pressure control

18. Distribution Statement

Unclassified - unlimited

19. Security Classif. (of this report)	20. Security Classif. (of this page)	21. No. of Pages	22. Price*
Unclassified	Unclassified	45	$3.00

*For sale by the Clearinghouse for Federal Scientific and Technical Information
Springfield, Virginia 22151

CONTENTS

ANALOG COMPUTER STUDY OF DESIGN PARAMETER EFFECTS ON THE STABILITY OF A DIRECT-ACTING GAS PRESSURE REGULATOR

by Miles O. Dustin

Lewis Research Center

SUMMARY

An analog computer study of a direct-acting gas pressure regulator is presented. The effect of regulator design parameters on stability, transient response, and steady-state accuracy were examined. The regulator used in the study is a single-stage, spring-loaded regulator used in the gas management system of a solar Brayton cycle power generator. The program was carried out in three parts:

1. An investigation of the effect of poppet stem friction, sensing orifice diameter, and output volume on the dynamic performance of a regulator with a linear spring and simple poppet
2. An investigation of the effect of an orifice in series with the poppet on regulator performance
3. An analog simulation of the Brayton cycle regulator which includes a nonlinear spring and orifice in series with the poppet and comparison of the simulation with performance curves taken from tests performed on the actual regulator

Poppet flow forces were determined experimentally. Flow forces were measured for both the simple poppet and for the poppet with a series orifice. It was found that the simple poppet flow forces work in a direction to aid in opening the poppet as the poppet is opened. This tends to make the regulator unstable. By adding an orifice in series with the poppet this effect is reversed. The force acts in a direction to close the poppet as it is opened, which has a stabilizing influence on the regulator. The orifice degrades steady-state regulation, however.

It was also found that with no friction on the poppet stem, a large spring rate was required to stabilize the regulator. The large spring rate causes poor steady-state regulation. However, if a small amount of friction is applied to the stem, the spring rate could be greatly reduced, resulting in improved regulation. Other factors which improve stability without affecting steady-state regulation are a decreased sensing orifice diameter and a larger output volume.

INTRODUCTION

The gas pressure regulator considered in this study was based on a regulator used in the gas management system in a solar Brayton cycle power generator. Since stability problems were encountered during the first checkout of the regulator, a study was carried out to determine those design parameters that affect the regulator stability and to determine the effect of these parameters on transient performance and steady-state regulation characteristics.

The simple, direct-acting, gas pressure regulator is used in almost every pneumatic system in use today. The modern industrial gas pressure regulator, having evolved over many years of application experience, provides good accuracy and stability characteristics over the range of pressures and flows of most commercial applications. However, the application of a given design to new pressure and flow conditions is uncertain and can result in unsatisfactory regulation.

The transient behavior of the simple hydraulic pressure regulator was analyzed by Gold and Otto in reference 1 using an electrical analogy technique. The steady-state characteristics of the simple gas regulator have been studied by Iberall in reference 2. Also, a dynamic analysis of the simple regulator has been done by Tsai and Cassidy in reference 3. Both linear and nonlinear problems were considered in the latter.

The difficulties encountered in making a dynamic analysis of the gas regulator are largely due to the nonlinearities of the equations describing the regulator. The nonlinearities include orifice flow through the metering valve, friction on the poppet stem, and the valve flow area as a function of stem position. The mathematical solution of the nonlinear equations describing the dynamic behavior is difficult and time consuming. It is usually necessary to linearize the equations about an operating point and to assume only small deviations of the variable from this operating point. It is therefore, not possible to study the transient behavior of the regulator to large changes in output flow.

The analog computer can be used to great advantage in this type of investigation. The nonlinear equations describing the regulator can be retained. Another important advantage of the analog computer is the ability to rapidly change the design parameters and to assess the effect of these changes on the dynamic performance of the regulator. This report describes an analog computer simulation of a simple, direct-acting gas regulator. The simulation includes the nonlinearities encountered in the real regulator.

The investigation was conducted in three parts:

(1) The first part, referred to as Case I in this report, considered the Brayton cycle regulator with two simplifications. A linear spring and a simple poppet metering valve were used. Changes were made in the design parameters to determine the effect of the changes on stability, transient performance, and steady-state regulation.

(2) To obtain good stability characteristics in the actual Brayton cycle gas regulator, the manufacturer added an orifice in series with the metering poppet valve. The second part of the study, or Case II, was to determine the effect of this orifice on the transient response and steady-state regulation of the regulator. All other fixed parameters such as bellows area, internal volumes, and valve area were the same as in the Case I study. As in the Case I study, changes were made in the design parameters to determine their effect on the regulator performance.

(3) The third part, Case III, was a simulation of the Brayton cycle gas regulator, with a nonlinear spring and the orifice in series with the poppet valve. The performance of the simulated regulator was then compared to performance tests made on the actual regulator by the regulator manufacturer.

REGULATOR DESCRIPTION

General Description

The simple, direct-acting gas regulator used for this study is shown schematically in figure 1. A bellows senses the regulated pressure P_r. (All symbols are defined in appendix A.) The bellows force, acting against a spring, adjusts the flow through the poppet valve to maintain the regulated pressure at the desired value. The desired pressure is set by the initial load on the spring.

This regulator has a balanced poppet valve. The poppet has been made insensitive to the regulator's supply pressure P_s by the addition of a small bellows attached to the bottom of the poppet. The regulated pressure P_r is supplied to this bellows by means of a bleed hole drilled through the poppet valve stem. This allows the regulated pressure to act on both ends of the poppet with equal areas, thus balancing the poppet.

Figure 2 more clearly illustrates the operating principle of the actual regulator. In this figure the pressure sensing bellows has been replaced by a piston. Pressure acts on areas A_1, A_2, and $A_3 - A_4$. These areas, which are separated by close clearances in figure 1, are separated by orifices A_{f2} and A_{f3} in figure 2. The balancing bellows in figure 1 has been replaced by a piston which has the same diameter as the valve seat. The series orifice used in the Case II and Case III studies is shown by dashed lines.

If only the regulated pressure and the initial spring force acted on the poppet stem, ideal pressure regulation would result. However, several other forces, which are functions of valve position and supply pressure, act on the system. These forces affect the steady-state accuracy of the regulator. These forces are listed and described below:

(1) An additional force is furnished by the spring, due to stroking the poppet. As the flow rate or supply pressure to the regulator changes, a new poppet position is required. Since the spring load must assume a new value, the regulated pressure must also change. This change in regulated pressure contributed to the steady-state offset of

the regulator. The magnitude of the force is determined by the poppet displacement and by the spring rate of the spring.

(2) Although the poppet is balanced, in that the same pressure is applied to both the top and bottom of the poppet, when flow occurs through the valve there is an increase in force on the top face of the poppet. This effect can be seen by referring to the two poppet conditons shown in the following sketch:

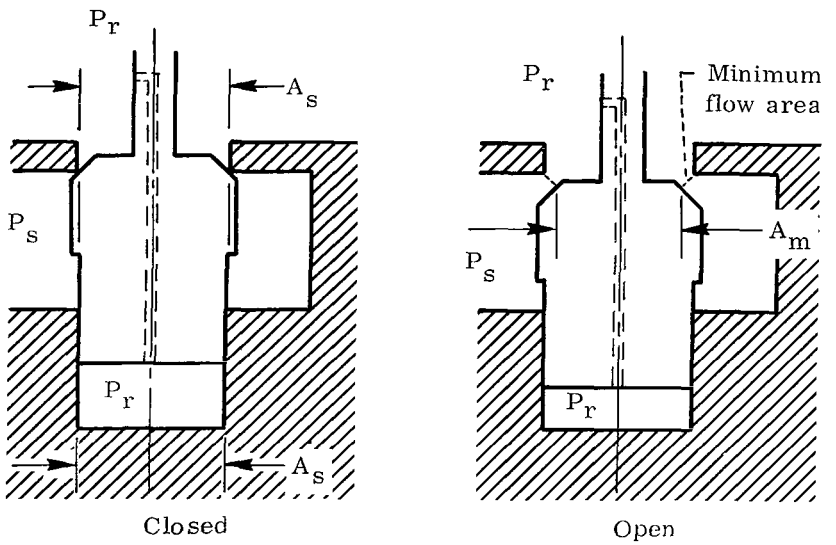

In the closed position the pressure P_r acts on the same area A_s on the top and bottom of the poppet. However, as the poppet opens, the location of the minimum flow area moves to a smaller diameter corresponding to A_m, as shown. Also, velocity through the poppet changes the static-pressure profile and allows P_s to act on a larger area. The net effect is to increase the force in a direction to open the poppet. (Additional information on poppet valve characteristics can be found in ref. 4.) The flow force is approximately proportional to valve stroke, just as is the spring force. However, the change in flow force is in the opposite direction, or in effect, is a negative spring rate. The spring rate of the spring has a stabilizing influence on the regulator, while the effective negative spring rate of the flow forces can contribute to instability in the regulator. However, the change in flow force does help to compensate for the steady-state offset due to the change in spring force when the valve assumes a new steady-state position. The flow force will cause the poppet stem to lose contact with the pressure sensing bellows and to open fully unless the stem is attached to the bellows (fig. 1). Another spring inside the balancing bellows can also be used to force the valve stem to remain in contact with the pressure sensing bellows.

(3) Sliding frictional forces on the valve stem resulting from guides on the stem can cause steady-state pressure errors. The frictional forces will also influence the stability characteristics of the regulator.

System Equations

The general equations developed in this section were used in all three parts of the study. Changes to the equations necessary to perform the various studies were made as required. Figure 3 defines the bellows areas used in the equations.

Dynamic equation. - The basic equation that describes the metering valve and bellows assembly dynamics is obtained by equating all forces acting on the assembly to zero. Positive forces are assumed to act upwards, and positive motion is assumed to be in the direction of opening the valve or downwards. The equation is

$$M\ddot{x} + K_s x + P_1A_1 + P_2A_2 + P_3(A_3 - A_4) - F_s - K_f x + F_f(\operatorname{sgn} \dot{x}) = 0 \qquad (1)$$

where

$M\ddot{x}$	force due to accelerating mass M (mass M is the mass of all moving parts.)
$K_s x$	additional spring force due to stroking metering poppet through distance x
P_1A_1, P_2A_2, $P_3(A_3 - A_4)$	pressure forces acting on bellows areas
F_s	initial force set on spring
$K_f x$	flow force on poppet valve (For this program flow force constant K_f was obtained experimentally for each supply pressure value. Appendix B describes the experimental procedure for obtaining the coefficients.)
$F_f(\operatorname{sgn} \dot{x})$	friction force on valve stem caused by valve stem support guides (It is assumed that the friction force is of constant value, that it acts upward when the stem motion is downward, and that it acts downward when the stem motion is upward, as shown in the following sketch.)

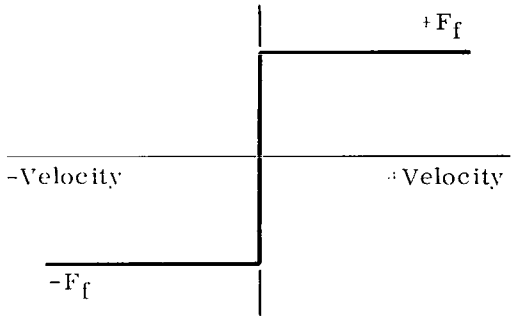

Continuity equation for main regulator flow. - If it is assumed that flow into volume V_1 is negligible, the continuity equation for flow into volume V_r may be written as

$$C_r \frac{dP_r}{dt} = \dot{m}_v - \dot{m}_o \tag{2}$$

where

$C_r \frac{dP_r}{dt}$ storage term for volume V_r (C_r is the pneumatic capacitance of volume V_r and is equal to V_r/kRT for an isentropic process. The effect of poppet stroke x on the capacitances C_r, C_1, C_2, and C_3 is small and is neglected throughout the report.)

$\dot{m}_v$ flow through metering poppet (It is assumed that flow through the valve is always choked.) For air,

$$\dot{m}_v = \frac{0.532\, C_f P_s A_v}{\sqrt{T}} \tag{3}$$

$$\left[\dot{m}_v = \frac{0.0400\, C_f P_s A_v}{\sqrt{T}}\right] \text{(for use with SI units)} \tag{3a}$$

where C_f is the valve flow coefficient and is assumed to be 0.8 (ref. 3), and A_v is a function of poppet displacement.

$\dot{m}_o$ regulator output flow which, since the output is always choked, is

$$\dot{m}_o = \frac{0.532\, C_f P_r A_o}{\sqrt{T}} \tag{4}$$

$$\left[\dot{m}_o = \frac{0.0400\, C_f P_r A_o}{\sqrt{T}}\right] \text{(for use with SI units)} \tag{4a}$$

Continuity equation for flow into volume V_1. - The continuity equation for the flow into volume V_1 can be expressed as

$$C_1 \frac{dP_1}{dt} = \dot{m}_1 - \dot{m}_2 + \rho_1 A_1 \dot{x} \tag{5}$$

where

$C_1 \frac{dP_1}{dt}$ storage term for volume V_1

m_1 flow into V_1 from volume V_r through orifice A_s (This flow is assumed to be incompressible, which can be said if the pressure drop between volume V_1 and volume V_r is small.)

$$\dot{m}_1 = A_s C_f \sqrt{2 g_o \rho_r |(P_r - P_1)|} \left[\text{sgn}(P_r - P_1)\right] \tag{6}$$

$$\dot{m}_2 = A_{f2} C_f \sqrt{2 g_o \rho_r |(P_1 - P_2)|} \left[\text{sgn}(P_1 - P_2)\right] \tag{7}$$

$\rho_r A_1 \dot{x}$ equivalent flow rate into volume V_1 because of the bellows motion

It is assumed that the densities ρ_1, ρ_2, ρ_3, and ρ_r are equal.

Continuity equation for flow into volume V_2. - In a similar manner, the continuity equation for flow into V_2 may be written as follows:

$$C_2 \frac{dP_2}{dt} = \dot{m}_2 - \dot{m}_3 + \rho_r A_2 \dot{x} \tag{8}$$

where

$$\dot{m}_3 = A_{f3} C_f \sqrt{2 g_o \rho_r |(P_2 - P_3)|} \left[\text{sgn}(P_2 - P_3)\right] \tag{9}$$

Continuity equation for flow into volume V_3. - In a similar manner, the continuity equation for flow into volume V_3 may be written as follows:

$$C_3 \frac{dP_3}{dt} = \dot{m}_3 + \rho_r (A_3 - A_4) \dot{x} \tag{10}$$

Metering valve flow area. - The change in the metering valve flow area A_v with respect to valve stroke x is dependent on the valve shape. The shape used in this program was that of the Brayton cycle regulator valve and is shown in figure 4. The flow area is a discontinuous function of stroke x, and may be expressed in general terms as follows:

When $0 < x < (r_p - r_v)/\cos\ \theta \sin\ \theta$

$$A_v = \pi\ x \sin\ \theta\ (2\ r_p - x \cos\ \theta \sin\ \theta) \tag{11}$$

When $(r_p - r_v)/\cos\ \theta \sin\ \theta < x < x_{max}$

$$A_v = \pi(r_p + r_v) \left\{ \left[x - \frac{(r_p - r_v)}{\tan\ \theta} \right]^2 + (r_p - r_v)^2 \right\}^{1/2} \tag{12}$$

ANALOG SIMULATION OF REGULATOR WITH SIMPLE POPPET - CASE I

Discussion

The first case studied was that of the regulator with a linear spring and a simple poppet metering valve. In terms of the system dynamic equation (eq. (1)), this simply means that the spring rate K_s is constant. The flow force coefficient K_f for the simple poppet was determined experimentally, as described in appendix B. Also, the sign of $K_f x$ is negative, as shown.

The simulation was performed on a general-purpose electronic analog computer. The specific equations used to construct the simulation are developed in appendix C.

The actual gas pressure regulator used in the Brayton cycle gas management system is required to regulate the system pressure under two output flow conditions. The transient responses conducted on the analog simulation were, therefore, made by switching the output flow orifices between areas of 0.10 and 0.004 square inch (0.65 and 0.026 cm^2). This is roughly equivalent to the acceptance tests performed on the actual regulators. Although the regulator was designed for ultimate use with a mixture of helium and xenon, the preliminary tests were conducted with nitrogen. The simulation was done with 530° R (290 K) air, which has nearly the same fluid dynamic properties as nitrogen at the same temperature.

Simulation Study Results

The study was designed to determine the effect of various system parameters on the stability of the regulator. The parameters involved were the sensing orifice diameter D_s, poppet stem friction F_f, output volume V_r, and supply pressure P_s. Table I gives a summary of conditions under which the study was conducted. The table also lists figures in which the results appear.

Effect of stem friction. - The effect of various amounts of friction on the regulator stability was determined in the following manner: With a fixed supply pressure P_s, sensing orifice diameter D_s, output volume V_r, and stem friction F_f, the system was made unstable by lowering the spring rate. The spring rate was then increased until the system was stable. It should be noted that the system could always be made stable with a sufficiently high spring rate. The system was defined as stable if oscillations were not sustained following a step change in output flow orifice area.

Figure 5 shows how the value of spring rate required to stabilize the system varies as a function of the stem friction F_f. From these curves it appears that small amounts of friction on the poppet stem tend to stabilize the regulator. This is particularly true when the sensing orifice is large. When the sensing orifice is small, the system is then insensitive to small amounts of friction but can be unstable if the friction becoms large.

Effect of sensing orifice diameter. - Figure 6 is a cross-plot of the data of figure 5 and shows how the amount of spring rate required to maintain a stable system varies as a function of sensing orifice diameter for various values of friction. These curves also show that, if the sensing orifice is large, the system can tolerate large amounts of stem friction. However, for orifice diameters larger than 0.070 inch (0.18 cm), at least a small amount of friction is very desirable to maintain stability.

Transient responses for various values of friction and sensing orifice diameter are shown in figures 7(a) to (e). These responses were all conducted with the same spring rate, supply pressure, and output volume. In figure 7(a) it can be seen that a system which is initially unstable can be stabilized by decreasing the size of the sensing orifice. However, if the orifice is made too small, large overshoots in the transient response can result.

Effect of output volume. - As the output volume is made larger, the system becomes more stable and can tolerate a lower spring rate. This effect is shown in figure 8, which is a plot of the spring rate necessary to stabilize the system as a function of the output volume. The largest sensing orifice diameter and smallest stem friction values were used to minimize their damping effects. It is desirable to operate the regulator with a minimum system spring rate, since this results in minimum steady-state regulation offset. Figure 9 shows the transient response of the system to step changes in output flow orifice area for various output volumes.

Effect of supply pressure. - With a linear spring, the regulator's ability to maintain a constant regulated pressure is greatly affected by supply pressure. This effect is shown in figure 10, which shows the transient response for step changes in output flow for several supply pressures. Since the gain of the poppet valve is a direct function of supply pressure, the regulator with a linear spring is more stable at low supply pressures. This means that the value of spring rate must be selected to give good stability at the highest supply pressure. This results in poor regulation or greater offset at low supply pressures, as shown in the figure. The ideal system should have a nonlinear spring

rate in which the rate changes as a function of stem position. When the poppet is nearly closed, which is the case for high supply pressure, the rate would be high. When the supply pressure is low and the poppet valve is further open, the spring rate would be lower. As will be shown later, this was done in the actual gas regulator considered in Case III.

ANALOG SIMULATION OF REGULATOR WITH ORIFICE IN SERIES WITH POPPET VALVE - CASE II

Discussion

During the initial checkout of the Brayton cycle gas pressure regulators, the manufacturer found that the regulators could be made stable by adding an orifice in series with the poppet valve. The orifice was placed downstream of the poppet valve, as shown in the inset of figure 1. The orifice area was 0.041 square inch (0.26 cm^2). This part of the analog study was to investigate the effect of the series orifice on regulator stability, transient response, and steady-state regulation. The effect of adding the orifice can be seen by referring to the inset of figure 1. The orifice produces a restriction in the normal poppet flow such that the pressure on top of the poppet face varies as a function of poppet stroke if the regulated pressure P_r is constant. The pressure on top of the poppet is fed to the bottom of the poppet and acts in an upward direction on the poppet. However, the area under the poppet is greater than the area on top of the poppet by an amount equal to the poppet stem. Thus, a net force is created that increases in an upward direction as the poppet is opened. The effect is in the same direction as the incremental spring force on the poppet and is in a direction to improve the regulator stability. The value of the flow force coefficient K_f was determined experimentally, as described in appendix B. In equation (1), the addition of the series orifice causes the sign on the $K_f x$ term to be positive.

Simulation Study Results

The study to determine the effect of the orifice in series with the poppet was conducted on the analog computer in a manner similar to the Case I tests wherein the simple poppet was used. That is, the output orifice areas were switched back and forth between areas of 0.10 and 0.004 square inch (0.65 and 0.026 cm^2). (A summary of conditions under which the study was conducted is given in table I.)

Effect of supply pressure and friction. - An important difference in the behavior of the regulator with the series orifice was that the regulator was nearly always stable, even with very low spring rates. Also, since the value of the flow force coefficient K_f increases with the supply pressure, the regulator is now more stable at high supply pressures. This effect can be seen by comparing the transient response curves shown in figures 11(a) to (c), which show transient behavior of the simulated regulator for various supply pressures and amounts of stem friction. The effect of stem friction on the performance of the regulator is also shown. If the regulator is quite unstable with no friction, as shown in the top trace of figure 11(a), additional friction increases the amplitude of the oscillations. However, if the regulator is only slightly unstable, as shown in figure 11(b), a small amount of friction stabilizes the regulator. If additional friction is present, the regulator output can assume additional error within limits determined by the friction value. The band of this additional error will be equal to the frictional force divided by the effective area of the bellows. The effective area of the bellows used in this study was 2.0 square inches (13 cm^2). Therefore, the output pressure can be ±5.0 psi (3.4 N/cm^2) from the zero friction output value if the stem friction is 10 pounds force (44 N).

Effect of sensing orifice diameter. - The effect of the sensing orifice diameter on the transient response to step changes in output flow is shown in figures 12(a) to (c). The effect is about the same as shown before for the simple poppet simulation. A system that is initially unstable can be stabilized by decreasing the sensing orifice size. However, if the orifice is made too small, large overshoots can result.

Effect of output volume. - Figures 13(a) to (c) show the effect of increasing the output volume. The effect is to make the system more stable. The system time constant, however, is increased.

ANALOG SIMULATION OF BRAYTON CYCLE REGULATOR - CASE III

Discussion

The first two parts of this study, Case I and Case II, evaluated on the analog computer the effect of many of the regulator design parameters on the stability, transient response, and regulation capabilities of the regulator. Many of these effects were also determined experimentally by the Brayton cycle gas regulator manufacturer during development and early checkout of the regulators. In addition to stabilizing the regulator by adding an orifice in series with the metering poppet valve and determining the optimum sensing orifice size, the regulator manufacturer installed a nonlinear spring. The effect of the nonlinear spring was to improve the low-supply-pressure offset by reducing the

spring rate at large poppet openings. This was done in the actual regulator by using a Bellville-type spring which has nonlinear characteristics. The nonlinear spring characteristics shown in figure 14 were added to the analog simulation of the regulator by the addition of a diode function generator. The regulator manufacturer measured the spring force as a function of valve stroke in an assembled regulator. The value of stem friction was arbitrarily chosen as 0.20 pound force (0.88 N) for the simulation.

Simulation Study Results

Figures 15 (a) to (c) show comparisons of simulated regulator performance with the actual regulator performance. The traces representing the actual regulator performance were redrawn from a light-beam oscillograph record. They were, therefore, expanded both in amplitude scale and time scale to match the analog simulation scales. They should, therefore, not be considered as accurate reproductions. Those features that are accurate are the magnitudes of the steady-state pressure levels for both high and low flows, the magnitudes of the pressure peaks, and the time for the pressure to reach the steady-state value following a transient. Only these factors will be considered in the discussion that follows. A summary of conditions under which the study was conducted is given in table I.

Figure 15(a) compares the simulated regulator responses to step changes in output flow with similar responses of the actual regulator when the output volume was 100 cubic inches (1600 cm^3) for both. The simulated regulator curves follow the same general shape as the actual regulator. However, the actual regulator exhibited a higher oscillation frequency. The overshoots when switching to low flow for the simulated regulator are higher than for the actual regulator. High overshoots were generally characteristic of small sensing orifice holes. This effect is demonstrated in figure 12(a). This could mean that the actual flow coefficient was greater than the 0.7 value used in the simulation. The offset was greater for the simulated regulator than for the actual regulator. This means that the effective spring rate was higher in the simulation. The effective spring rate is a combination of the spring rate of the spring and the effect of the flow force on the poppet.

In figure 15(b) the output volume was increased from 100 cubic inches (1600 cm^3) to 400 cubic inches (6500 cm^3) for both regulators. The overshoots are still larger in the simulated regulator, but it is not as noticeable with the larger output volume. Both regulators are more stable, as expected.

Figure 15(c) shows the effect of increasing the sensing orifice size from 0.025 inch (0.064 cm) to 0.036 inch (0.091 cm), while keeping the output volume at 400 cubic inches (6500 cm^3). The simulated regulator has become more stable, while the actual regulator

has become less stable. As can be seen by referring to figure 6, the effect of changing the sensing orifice size depends upon the amount of stem friction. The value of stem friction for the simulation was chosen arbitrarily as 0.2 pound force (0.88 N), which may not agree with the actual regulator. This means that changing the sensing orifice size may not affect the simulation in the same manner as it affects the actual regulator.

SUMMARY OF RESULTS

A single-stage, gas pressure regulator consisting of a spring-loaded, bellows-actuated poppet valve was analyzed. System equations were written and simulated on the analog computer. The computer simulation was used to determine the effects of the significant design parameters such as spring stiffness, stem friction, sensing orifice size, and output volume on the transient behavior of the regulator. Also represented in the simulation were certain design refinements such as a nonlinear spring, a poppet pressure balancing bellows and a downstream orifice between the poppet metering area and the pressure sensing orifice. The effects of the significant design parameters and refinements on regulator stability, response, and steady-state accuracy were demonstrated. Results from the analog computer simulation were compared with experimental results for a regulator designed for pressurizing a solar Brayton cycle space power generator. The mathematical model and computer circuit presented can be readily adapted to other similar regulator designs. Also, the trends pointed out could be used as guidelines by designers for making judicious improvements in the performance of regulator designs without recourse to detailed analysis.

The following is a brief summary of the results of the study:

1. An increase in system spring rate tends to improve stability; however, the regulating ability of the regulator is decreased.

2. Decreasing the size of the sensing orifice tends to stabilize the regulator until an optimum orifice size is reached. Further reduction can cause instability, especially if the stem friction is great. It has no effect on the steady-state offset.

3. Increasing the regulator's supply pressure can cause instability with a fixed spring rate. A nonlinear spring can provide good stability at all supply pressures with minimum steady-state offset.

4. An orifice in series with the metering poppet valve can be used to improve the regulator's stability. The effect is similar to the nonlinear spring in that the orifice creates a stabilizing force which is greatest at high supply pressures. It also increases the steady-state offset.

5. A small amount of friction can be of great value in stabilizing the regulator, especially if the sensing orifice is too large to have a stabilizing effect. Too much friction,

however, can cause instability if the sensing orifice diameter is small. It can also cause the regulator to have a dead band whose width is a function of the friction value.

6. Increasing the output volume has a definite stabilizing effect. The only detrimental effect of increasing the volume is that the time constant of the system is increased.

Lewis Research Center,
National Aeronautics and Space Administration,
Cleveland, Ohio, November 30, 1970,
720-03.

APPENDIX A

SYMBOLS

A	area, $in.^2$; cm^2
A_{f2}	flow area between volume V_1 and volume V_2 (see figs. 1 and 2), $in.^2$; cm^2
A_{f3}	flow area between volume V_2 and volume V_3 (see figs. 1 and 2), $in.^2$; cm^2
A_m	area of poppet measured at minimum flow area, $in.^2$; cm^2
A_o	area of output orifice (see fig. 1), $in.^2$; cm^2
A_p	area of poppet seat (see fig. 1), $in.^2$; cm^2
A_s	area of sensing orifice (see fig. 1), $in.^2$; cm^2
A_{st}	stem area used in poppet valve tests, $in.^2$; cm^2
A_v	metering area of poppet (see fig. 1), $in.^2$; cm^2
C	capacitance, $(in.^2)(lbm)/lbf$; $(cm^2)(kg)/N$
C_f	flow coefficient
D_s	diameter of sensing orifice (see fig. 1), in.; cm
F_f	friction force, lbf; N
F_m	measured poppet force, lbf; N
F_s	spring force, lbf; N
g_o	gravitational constant, 386 $(lbm)(in.)/(lbf)(sec^2)$; 100 $(kg)(cm)/(N)(sec^2)$
K_f	flow force coefficient, lbf/in.; N/cm
K_s	spring rate, lbf/in.; N/cm
k	ratio of specific heats
M	mass, $lbf\text{-}sec^2/in.$; $N\text{-}sec^2/cm$
$\dot{m}$	mass flow rate (see fig. 1), lbm/sec; kg/sec
$\dot{m}_h$	mass flow rate from output orifice under high-flow-rate conditions (see fig. 4), lbm/sec; kg/sec
$\dot{m}_l$	mass flow rate from output orifice under low-flow-rate conditions (see fig. 4), lbm/sec; kg/sec
$\dot{m}_v$	mass flow rate through metering poppet (see fig. 1), lbm/sec; kg/sec
$\dot{m}_o$	mass flow rate through output orifice (see fig. 1), lbm/sec; kg/sec

P	pressure, psia; N/cm^2
R	gas constant, in.-lbf/(lbm)(^oR); cm-N/(kg)(K)
r_p	radius of poppet valve seat (see fig. 4), in.; cm
r_v	inside radius of bevel on poppet (see fig. 4), in.; cm
sgn[ ]	sign of [ ]
T	temperature of gas, ^oR; K
t	time, sec
V	volume, $in.^3$; cm^3
x	stroke, in.; cm
$\dot{x}$	velocity, in./sec; cm/sec
$\ddot{x}$	acceleration, $in./sec^2$; cm/sec^2
θ	poppet bevel angle (see fig. 4), deg
ρ	density, $lbm/in.^3$; kg/cm^3

Subscripts:

b	pressure balancing bellows
f	flow
max	maximum
r	conditions in output volume (see fig. 1)
s	supply
1, 2, 3, 4	conditions under various bellows areas (see figs. 1 and 2)

APPENDIX B

DETERMINATION OF FLOW FORCE COEFFICIENTS

The flow force appearing in equation (1) as $K_f x$, results from increased pressure loading on the top of the poppet as it is opened. In the closed position, equal pressures act on the top and bottom of the poppet. However, as the valve moves open, the minimum flow area moves to a smaller diameter. This allows the supply pressure to act on a larger area and the regulated pressure to act on a smaller area, resulting in a net increase in downward force on the poppet. Reference 4 gives emperical flow force equations derived from experimental data of reference 3 for several poppet designs. In this study, however, it was decided to obtain the flow forces experimentally because of the unusual poppet design involved.

A special test fixture, shown in figure 16, was built for obtaining the flow forces for both the simple poppet and for the poppet in series with an orifice. The orifice sleeve was soldered into the valve seat after the tests on the simple poppet configuration were completed.

The poppet opening was varied by means of an adjustment screw on the force cell. The regulated pressure was controlled by means of a pneumatic operated valve on the output line. The regulated pressure was measured with a pressure transducer and the pressure was regulated by a proportional-plus-integral electronic controller. The output of the controller was converted to a pneumatic signal by means of a torque-motor-actuated, three-way valve.

Tests were conducted in the following manner: The main valve from the nitrogen bottles was initially closed and the six valves on the nitrogen bottles were opened. The poppet opening was adjusted to the desired value. The main valve was then opened suddenly, discharging the nitrogen bottles through the poppet valve fixture. Variables recorded on an eight-channel strip-chart recorder include (1) supply pressure P_s; (2) pressure which normally would be in the pressure balancing bellows P_b, (3) regulated pressure P_r, and (4) force on the load cell F_m.

To convert the force measured during these tests to an equivalent force for use in the simulation, it was necessary to add to the measured force F_m a force equal to the stem area A_{st} times the regulated pressure P_r. It is also necessary to subtract a force equal to the effective area of the balancing bellows times the measured bellows pressure P_b. Figure 17(a) shows the resulting flow force plotted as a function of poppet stroke for the simple poppet. Figure 17(b) shows the flow force as a function of poppet stroke for the poppet in series with the orifice. Values of flow force coefficient K_f were taken as the slopes of these curves at the operating poppet opening value for the maximum regulator flow condition. The curves shown as dashed lines were extrapolated

from data taken at lower pressures. Even though the nitrogen bottles were initially charged at 2000 psig (1380 N/cm^2), the supply pressure at the fixture under flowing conditions rarely exceeded 1200 psig (830 N/cm^2) because of pressure losses through the valves on the bottles.

APPENDIX C

DEVELOPMENT OF SPECIFIC SYSTEM EQUATIONS FOR ANALOG SIMULATION

The general equations used to describe the gas pressure regulator are given in the main text in the section System Equations. The specific equations used to construct the analog computer wiring diagram, figure 18, will be developed in this appendix. The equations appearing in brackets are for use with the SI units as shown in the symbol list (appendix A). Potentiometer settings are listed in table II.

Dynamic Equation

The general equation describing the dynamics of the metering valve and bellows assembly is given by equation (1):

$$M\ddot{x} + K_s x + P_1 A_1 + P_2 A_2 + P_3(A_3 - A_4) - F_s - K_f x + F_f(\operatorname{sgn} \dot{x}) = 0 \qquad (1)$$

The coefficients for this equation were obtained directly from the manufacturer's detailed drawings for the regulator and are as follows:

$$M = 1.86\times10^{-3} \text{ lbf-sec}^2/\text{in.} \ (3.26\times10^{-3} \text{ N-sec}^2/\text{cm})$$

$$A_1 = 0.770 \text{ in.}^2 \ (4.96 \text{ cm}^2)$$

$$A_2 = 0.244 \text{ in.}^2 \ (1.57 \text{ cm}^2)$$

$$A_3 - A_4 = 0.969 \text{ in.}^2 \ (6.25 \text{ cm}^2)$$

$$F_s = 360 \text{ lbf } (1600 \text{ N})$$

$$F_f = \text{Variable}$$

$$K_s = \text{Variable}$$

K_f is a function of x and P_s and must be adjusted in accordance with experimental data for each P_s value. Using these values, equation (1) can be written

$$-\ddot{x} = (0.538\times10^{3}K_s)x + (0.414\times10^{3})P_1 + (0.131\times10^{3})P_2 + (0.520\times10^{3})P_3 - 194\times10^{3}$$

$$- (0.538\times10^{3})K_f\dot{x} + (0.538\times10^{3})F_f(\text{sgn }\dot{x}) \qquad \text{(C1)}$$

$$\left[\ddot{x} = (0.307\times10^{3}K_s)x + (1.52\times10^{3})P_1 + (0.481\times10^{3})P_2 + (1.92\times10^{3})P_3 - 490\times10^{3}\right.$$

$$\left. - (0.307\times10^{3})K_f + (0.307\times10^{3})F_f(\text{sgn }\dot{x})\right] \qquad \text{(C1a)}$$

Continuity Equation for Main Regulator Flow

The general equation for flow into volume V_r is

$$C_r\frac{dP_r}{dt} = \dot{m}_v - \dot{m}_o \qquad (2)$$

Since $C_r = V_r/kRT$, V_r = 122 cubic inches (2000 cm^3), and $T = 530^{\circ}$ R (290 K), $C_r = 2.56\times10^{-4}$ $(in.^2)(lbm)/lbf\left[1.68\times10^{-4}\ (cm^2)(kg)/N\right]$. Also, for choked flow through the poppet and a flow coefficient of 0.8,

$$\dot{m}_v = 1.85\times10^{-2}A_vP_s \qquad \text{(C2)}$$

$$\left[\dot{m}_v = 1.89\times10^{-3}A_vP_s\right] \qquad \text{(C2a)}$$

For flow through the maximum output flow orifice area of 0.10 square inch (0.65 cm^2) with a flow coefficient of 0.6, equation (2) becomes

$$\frac{dP_r}{dt} = 0.723\times10^{2}A_vP_s - 5.42P_r \qquad \text{(C3)}$$

$$\left[\frac{dP_r}{dt} = 11.2A_vP_s - 5.42P_r\right] \qquad \text{(C3a)}$$

For flow through the minimum orifice area of 0.004 square inch (0.026 cm^2), equation (2) becomes

$$\frac{dP_r}{dt} = 0.723\times10^2 A_v P_s - 0.217 P_r \tag{C4}$$

$$\left[\frac{dP_r}{dt} = 11.2 A_v P_s - 0.217 P_r\right] \tag{C4a}$$

When a change in output volume was investigated, equations (C3) and (C4) were altered to account for the change in C_r. This simply means that all coefficients in the equations are changed inversely proportional to the change in output volume.

Continuity Equation for Flow Into Volume V_1

The general equation for flow into volume V_1 is

$$C_1 \frac{dP_1}{dt} = \dot{m}_1 - \dot{m}_2 + \rho_1 A_1 \dot{x} \tag{5}$$

Since $C_1 = V_1/kRT$, $V_1 = 1.69$ cubic inches (27.7 cm^3), and $T = 530^o$ R (290 K), $C_1 = 3.55\times10^{-6}(in.^2)(lbm)/lbf \left[2.35\times10^{-6}(cm^2)(kg)/N\right]$.

The values of densities ρ_r, ρ_1, ρ_2, and ρ_3 were assumed constant and were calculated at the set regulated pressure of 180 psia (124 N/cm^2). The area A_1 was 0.77 square inch (4.96 cm^2). Substituting these values into equation (5) yields

$$\frac{dP_1}{dt} = (2.82\times10^5)\dot{m}_1 - (2.82\times10^5)\dot{m}_2 + (1.15\times10^2)\dot{x} \tag{C5}$$

$$\left[\frac{dP_1}{dt} = (4.26\times10^5)\dot{m}_1 - (4.26\times10^5)\dot{m}_2 + (0.311\times10^2)\dot{x}\right] \tag{C5a}$$

Flow $\dot{m}_1$ into V_1 through the sensing orifice is assumed to be incompressible and may be obtained from equation (6):

$$\dot{m}_1 = A_s C_f \sqrt{2 g_o \rho_r |(P_r - P_1)|}\ [\mathrm{sgn}(P_r - P_1)] \tag{6}$$

Substituting in specific values of ρ_r computed at 180 psia (124 N/cm^2) and an assumed value of C_f of 0.7,

$$\dot{m}_1 = 0.45A_s\sqrt{|(P_r - P_1)|}\,[sgn(P_r - P_1)] \tag{C6}$$

$$\left[\dot{m}_1 = 3.8\times10^{-2}A_s\sqrt{|(P_r - P_1)|}\,[sgn(P_r - P_1)]\right] \tag{C6a}$$

Flow $\dot{m}_2$ from volume V_1 into V_2 is obtained from equation (7)

$$\dot{m}_2 = A_{f2}C_f\sqrt{2g_o\rho_r|(P_1 - P_2)|}\,[sgn(P_1 - P_2)] \tag{7}$$

Substituting a flow area A_{f2} of 0.145 square inch (0.935 cm^2) taken from manufacturers' drawings, equation (7) becomes

$$\dot{m}_2 = 0.0653\sqrt{|(P_1 - P_2)|}\,[sgn(P_1 - P_2)] \tag{C7}$$

$$\left[\dot{m}_2 = 3.56\times10^{-2}\sqrt{|(P_1 - P_2)|}\,[sgn(P_1 - P_2)]\right] \tag{C7a}$$

Continuity Equation for Flow Into Volume V_2

The continuity equation for flow into volume V_2 is

$$C_2\frac{dP_2}{dt} = \dot{m}_2 - \dot{m}_3 + \rho_r A_2\dot{x} \tag{8}$$

Volume V_2 measures 0.0127 cubic inch (0.208 cm^3), which results in a value for C_2 of 2.67×10^{-8} (in.^{2})(lbm)/lbf $\left[1.75\times10^{-8}\ (cm^2)(kg)/N\right]$. Substituting this value of C_2 and a value for A_2 of 0.244 square inch (1.57 cm^2) into equation (8) results in

$$\frac{dP_2}{dt} = (3.75\times10^7)\dot{m}_2 - (3.75\times10^7)\dot{m}_3 + (0.484\times10^4)\dot{x} \tag{C8}$$

$$\left[\frac{dP_2}{dt} = (5.70\times10^7)\dot{m}_2 - (5.70\times10^7)\dot{m}_3 + (0.131\times10^4)\dot{x}\right] \tag{C8a}$$

Flow $\dot{m}_3$ from volume V_2 into volume V_3 is obtained from equation (9):

$$\dot{m}_3 = A_{f3} C_f \sqrt{2 g_o \rho_r |(P_2 - P_3)|} \; [\text{sgn}(P_2 - P_3)] \tag{9}$$

With a measured flow area A_{f3} of 0.047 square inch (0.303 cm^2) equation (9) becomes

$$\dot{m}_3 = 0.0212 \sqrt{|(P_2 - P_3)|} \; [\text{sgn}(P_2 - P_3)] \tag{C9}$$

$$\left[\dot{m}_3 = 1.15 \times 10^{-2} \sqrt{|(P_2 - P_3)|} \; [\text{sgn}(P_2 - P_3)]\right] \tag{C9a}$$

Continuity Equation for Flow Into Volume V_3

The continuity equation for flow into volume V_3 is

$$C_3 \frac{dP_3}{dt} = \dot{m}_3 + \rho_r (A_3 - A_4) \dot{x} \tag{10}$$

Volume V_3 measures 0.112 cubic inch (1.84 cm^3), which results in a value of C_2 of 0.235×10^{-6} $(in.^2)(lbm)/lbf$ $\left[0.155 \times 10^{-6} \; (cm^2)(kg)/N\right]$. Substituting this value for C_3 and the correct values for ρ_r and $A_3 - A_4$ into equation (10) gives

$$\frac{dP_3}{dt} = (4.26 \times 10^6) \dot{m}_3 + (2.18 \times 10^3) \dot{x} \tag{C10}$$

$$\left[\frac{dP_3}{dt} = (6.47 \times 10^6) \dot{m}_3 + (5.93 \times 10^2 \dot{x}\right] \tag{C10a}$$

REFERENCES

1. Gold, Harold; and Otto, Edward W.: An Analytical and Experimental Study of the Transient Response of a Pressure-Regulating Relief Valve in a Hydraulic Circuit. NACA TN 3102, 1954.

2. Iberall, A. S.: Static-Flow Characteristics of Single and Two-Stage Spring-Loaded Gas Pressure Regulators. Trans. ASME, vol. 76, no. 3, Apr. 1954, pp. 363-373.

3. Tsai, D. H.; and Cassidy, E. C.: Dynamic Behavior of a Simple Pneumatic Pressure Reducer. J. Basic Eng., vol. 83, no. 2, June 1961, pp. 253-264.

4. Andersen, Blaine W.: The Analysis and Design of Pneumatic Systems. John Wiley & Sons, Inc., 1967.

TABLE I. - SUMMARY OF CONDITIONS UNDER WHICH ANALOG COMPUTER STUDY WAS CONDUCTED FOR CASES I, II, AND III

Case	Objective	Supply pressure, P_s		Spring rate, K_s		Friction force, F_f		Output volume, V_r		Sensing orifice diameter, D_s		Figure
		psia	N cm^2	lbf in.	N cm	lbf	N	in.^{3}	cm^3	in.	cm	
I	Effect of friction force on stability	2000	1380	Varied	Varied	Varied	Varied	122	2000	Varied	Varied	5
	Effect of sensing orifice diameter on stability			Varied	Varied	Varied	Varied					6
	Effect of friction force and sensing orifice diameter on response			1235	2160	0	0					7(a)
						.20	.88					7(b)
						.40	1.78					7(c)
						2.0	8.8					7(d)
						10	44					7(e)
	Effect of output volume on stability			Varied	Varied	.20	.88	Varied	Varied	0.125	0.318	8
	Effect of output volume on response			1040	1820	.20	.88	Varied	Varied	.125	.318	9
	Effect of supply pressure on response	Varied	Varied	1560	2730	.20	.88	122	2000	.125	.318	10
II	Effect of friction force on response	300	207	100	175	Varied	Varied	122	2000	0.125	0.318	11(a)
		1000	690			Varied	Varied			.125	.318	11(b)
		2000	1380			Varied	Varied			.125	.318	11(c)
	Effect of sensing orifice diameter on response	300	207			0.20	0.88			Varied	Varied	12(a)
		1000	690							Varied	Varied	12(b)
		2000	1380							Varied	Varied	12(c)
	Effect of output volume on response	300	207					Varied	Varied	0.125	0.318	13(a)
		1000	690					Varied	Varied	.125	.318	13(b)
		2000	1380					Varied	Varied	.125	.318	13(c)
III	Effect of supply pressure on response	Varied	Varied	Nonlinear	Nonlinear	0.20	0.88	100	1600	0.025	0.064	15(a)
		Varied	Varied	Nonlinear	Nonlinear	.20	.88	400	6500	.025	.064	15(b)
		Varied	Varied	Nonlinear	Nonlinear	.20	.88	400	6500	.036	.091	15(c)

TABLE II. - POTENTIOMETER SETTINGS FOR GAS REGULATOR SIMULATION

Potentiometer	Setting	Potentiometer	Setting
1	0.100	18	0.282
2	.131	19	.115
3	.414	20	.282
4	.520	21	.100
5	[a].538×10^{-3}K$_s$	22	.180
5	[b].538	23	$\frac{F_f}{100 + F_f}$
6	.194		
7	.538		
8	.538×10^{-3}K$_f$	24	$\frac{F_f}{100 + F_f}$
9	.010		
10	.570	25	.197
11	.361×10^{-3}P$_s$	26	.375
12	5.55×10$^{-4}\dot{m}_h/C_r$	27	.048
13	5.55×10^{-4}m$_l$/C$_r$	28	.375
14	.100	29	.018
15	.180	30	.218
16	.100	31	.426
17	33.9 D$_s^2$	32	.180
		33	.202

[a]Case I and Case II only.

[b]Case III only.

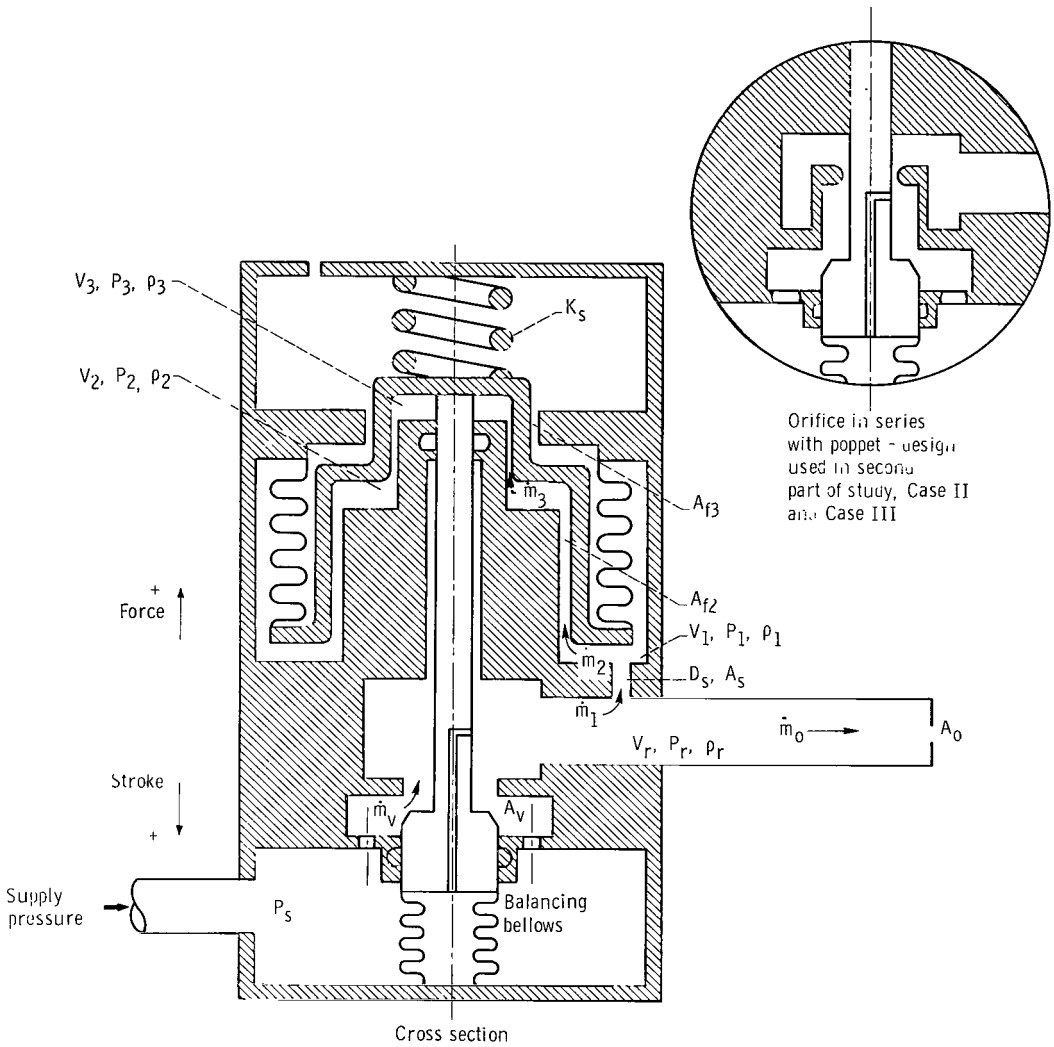

Figure 1. - Gas pressure regulator used in first part of study. Case I simple poppet is shown. Inset shows design of orifice in series with poppet, as used in Case II and Case III parts of study.

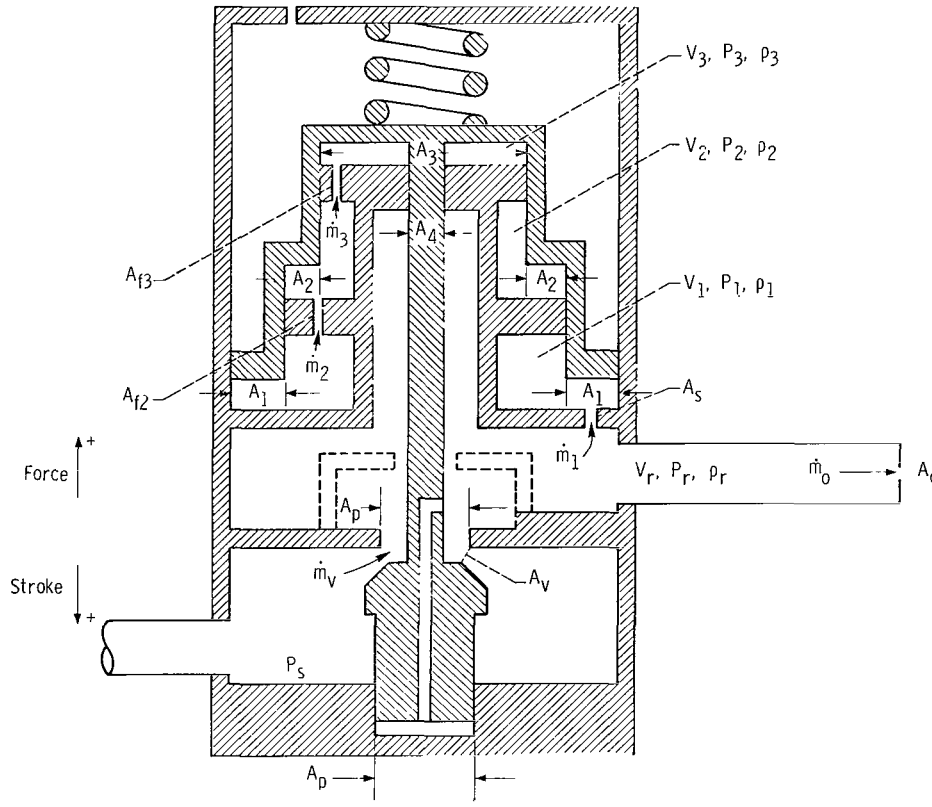

Figure 2. - Simplified schematic of gas pressure regulator.

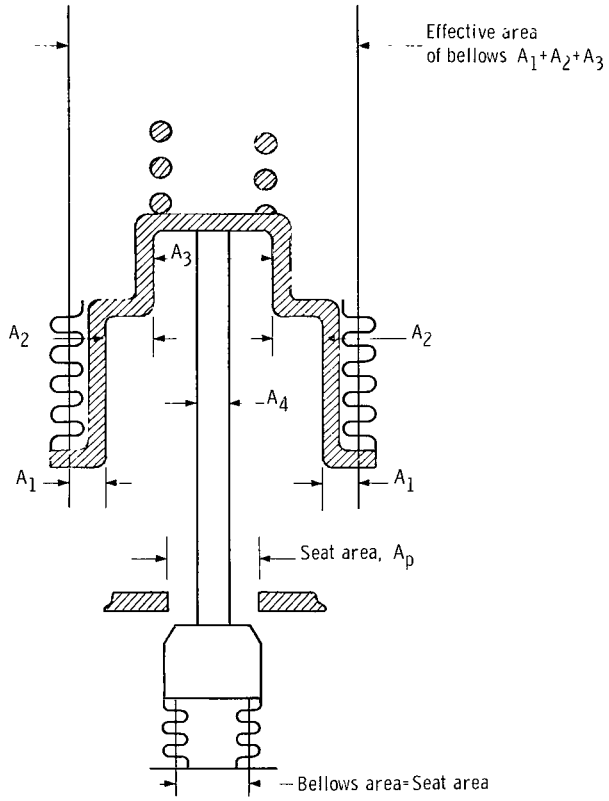

Figure 3. - Schematic of bellows assembly showing areas used in developing dynamic equation.

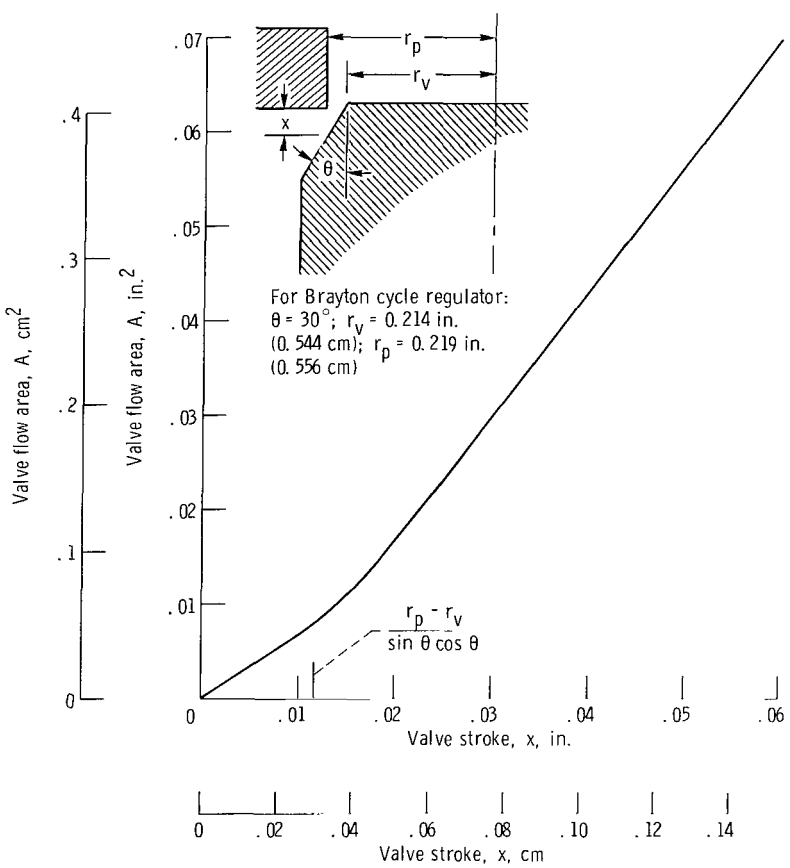

Figure 4. - Metering valve flow area as function of valve stroke.

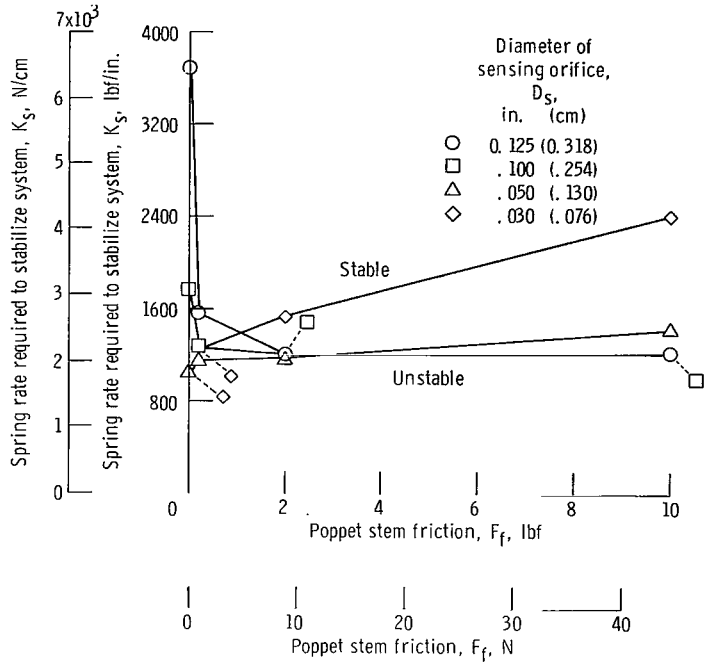

Figure 5. - Effect of poppet stem friction on regulator stability. Case I, simple poppet; supply pressure, 2000 psia (1380 N/cm^2); output volume, 122 cubic inches (2000 cm^3).

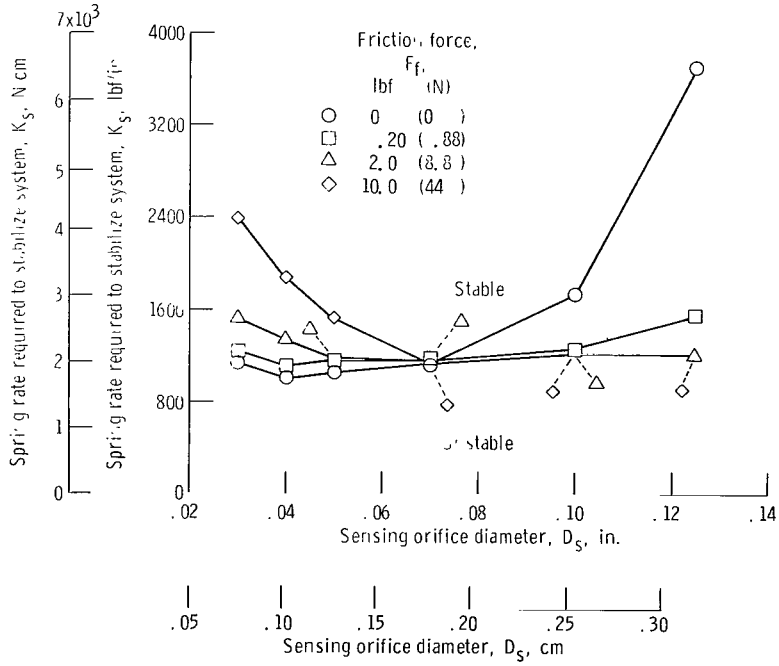

Figure 6. - Effect of sensing orifice size on regulator stability. Case I, simple poppet; supply pressure, 2000 psia (1380 N/cm^2); output volume, 122 cubic inches (2000 cm^3).

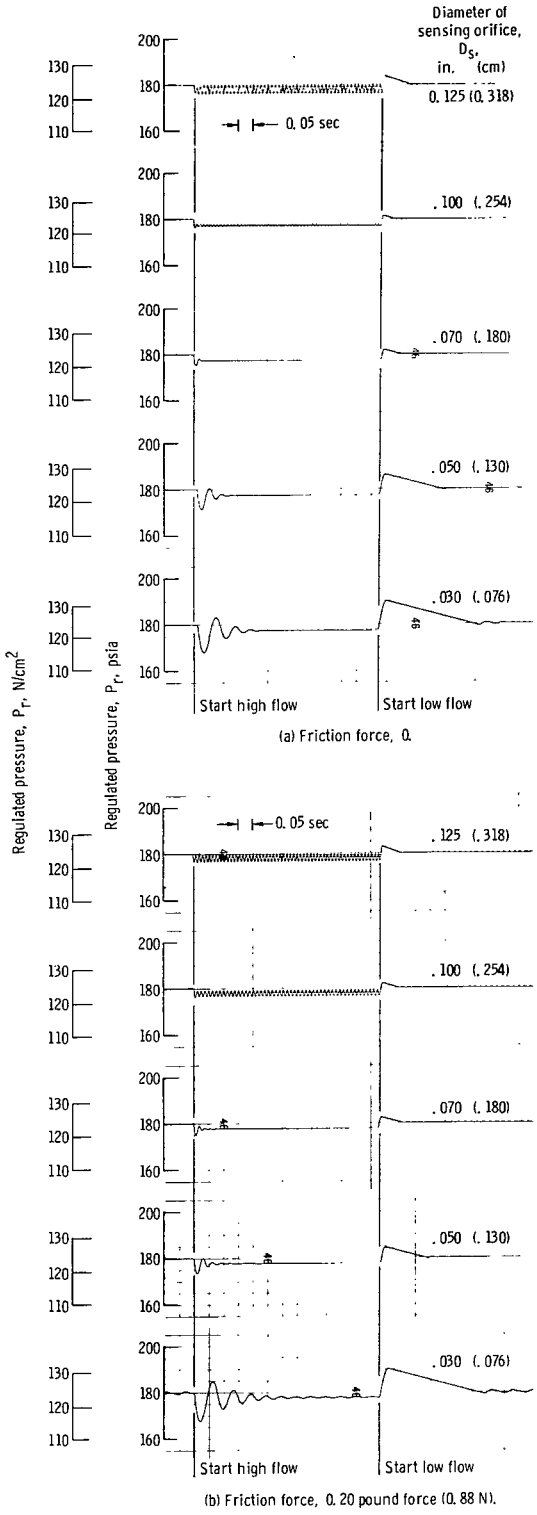

Figure 7. - Simulated regulator response to step changes in output flow orifice area for various sensing orifice diameters. Case I, simple poppet; supply pressure, 2000 psia (1380 N/cm^2); output volume, 122 cubic inches (2000 cm^3); spring rate, 1235 pound force per inch (2160 N/cm).

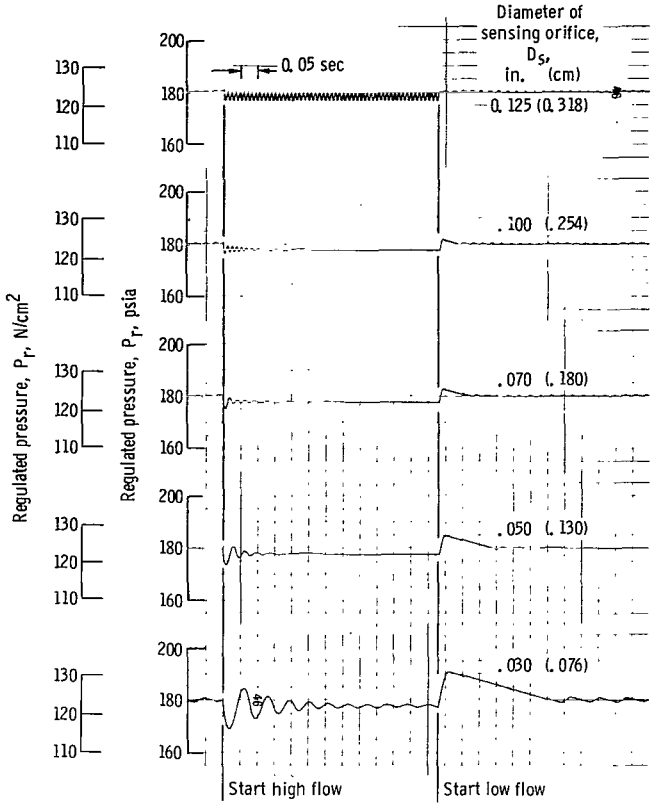

(c) Friction force, 0.40 pound force (1.78 N).

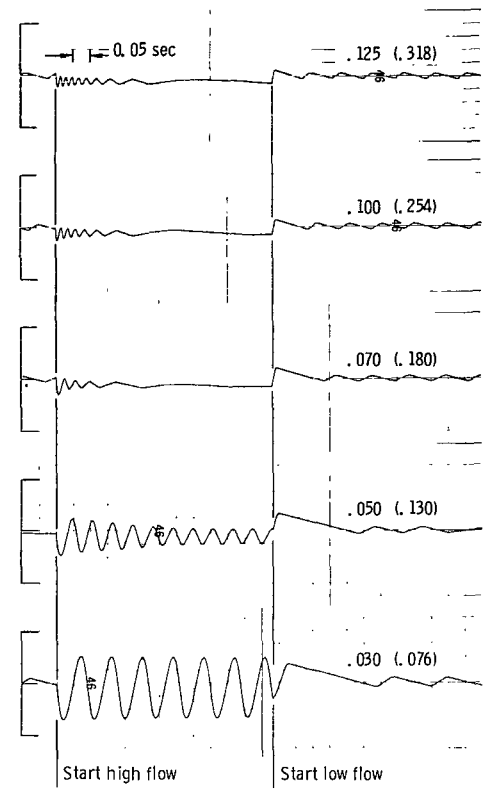

(d) Friction force, 2.0 pounds force (8.8 N).

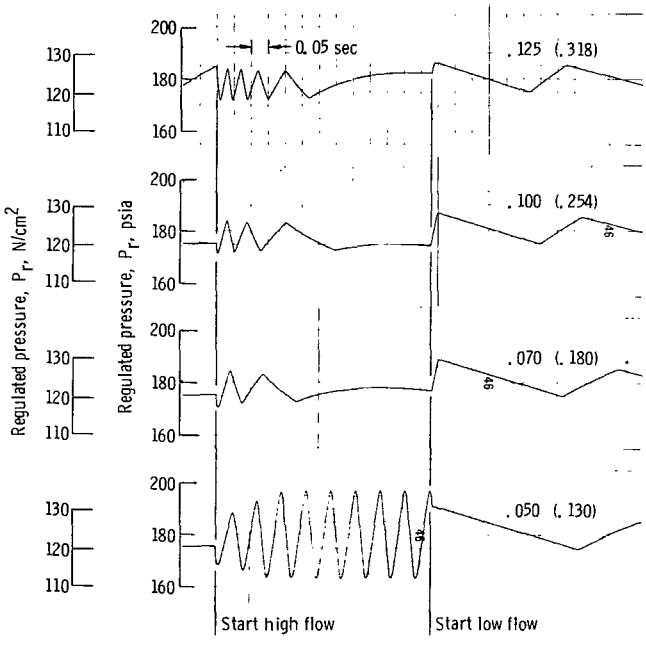

(e) Friction force, 10.0 pounds force (44 N).

Figure 7. - Concluded.

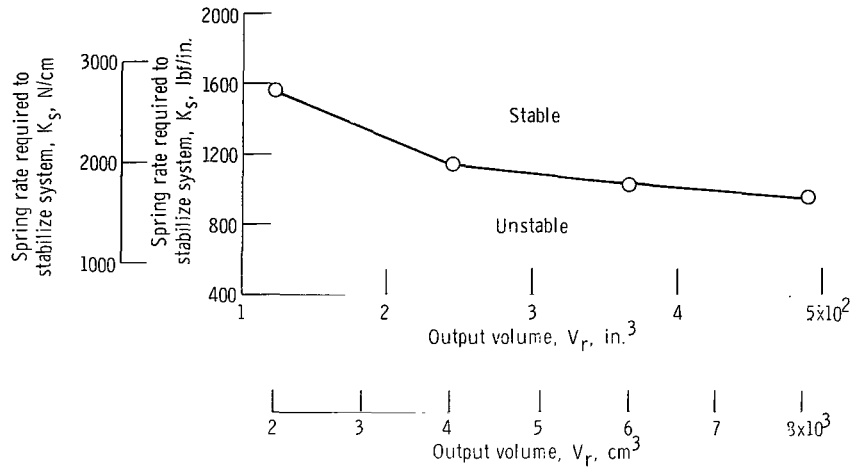

Figure 8. - Effect of output volume on regulator stability. Case I, simple poppet; supply pressure, 2000 psia (1380 N/cm^2); sensing orifice diameter, 0.125 inch (0.318 cm); stem friction, 0.2 pound force (0.88 N).

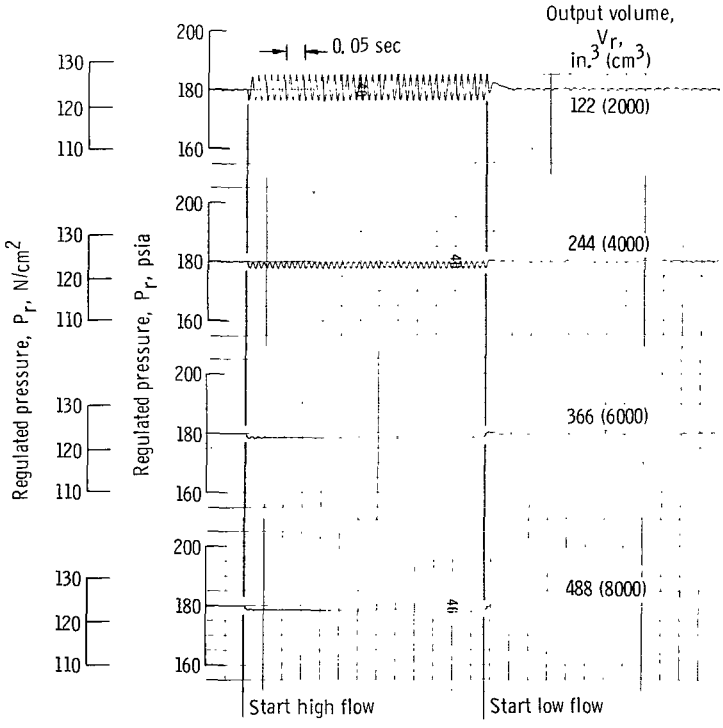

Figure 9. - Simulated regulator response to step changes in output flow orifice area for various values of output volume. Case I, simple poppet; supply pressure, 2000 psia (1380 N/cm); stem friction, 0.2 pound force (0.88 N); sensing orifice diameter, 0.125 inch (0.318 cm).

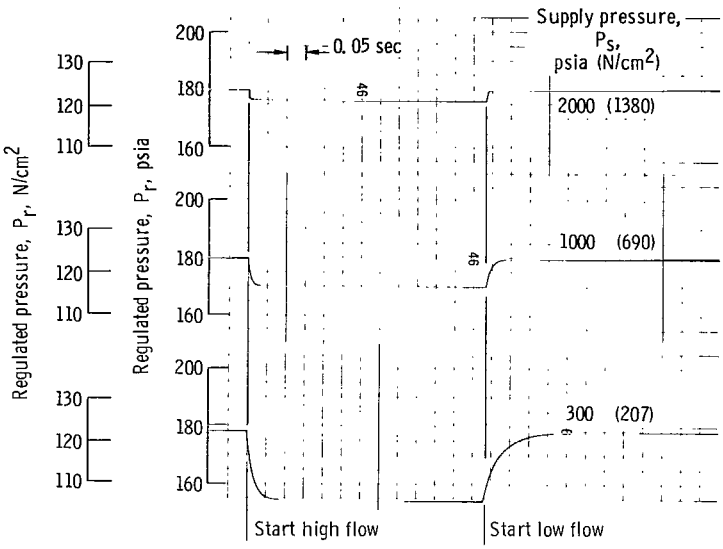

Figure 10. - Simulated regulator response to step changes in output flow orifice area for various values of supply pressure. Case I, simple poppet; spring rate, 1560 pounds force per inch (2730 N/cm^2); stem friction, 0.2 pound force (0.88 N); sensing orifice diameter, 0.125 inch (0.318 cm); output volume, 122 cubic inches (2000 cm^3).

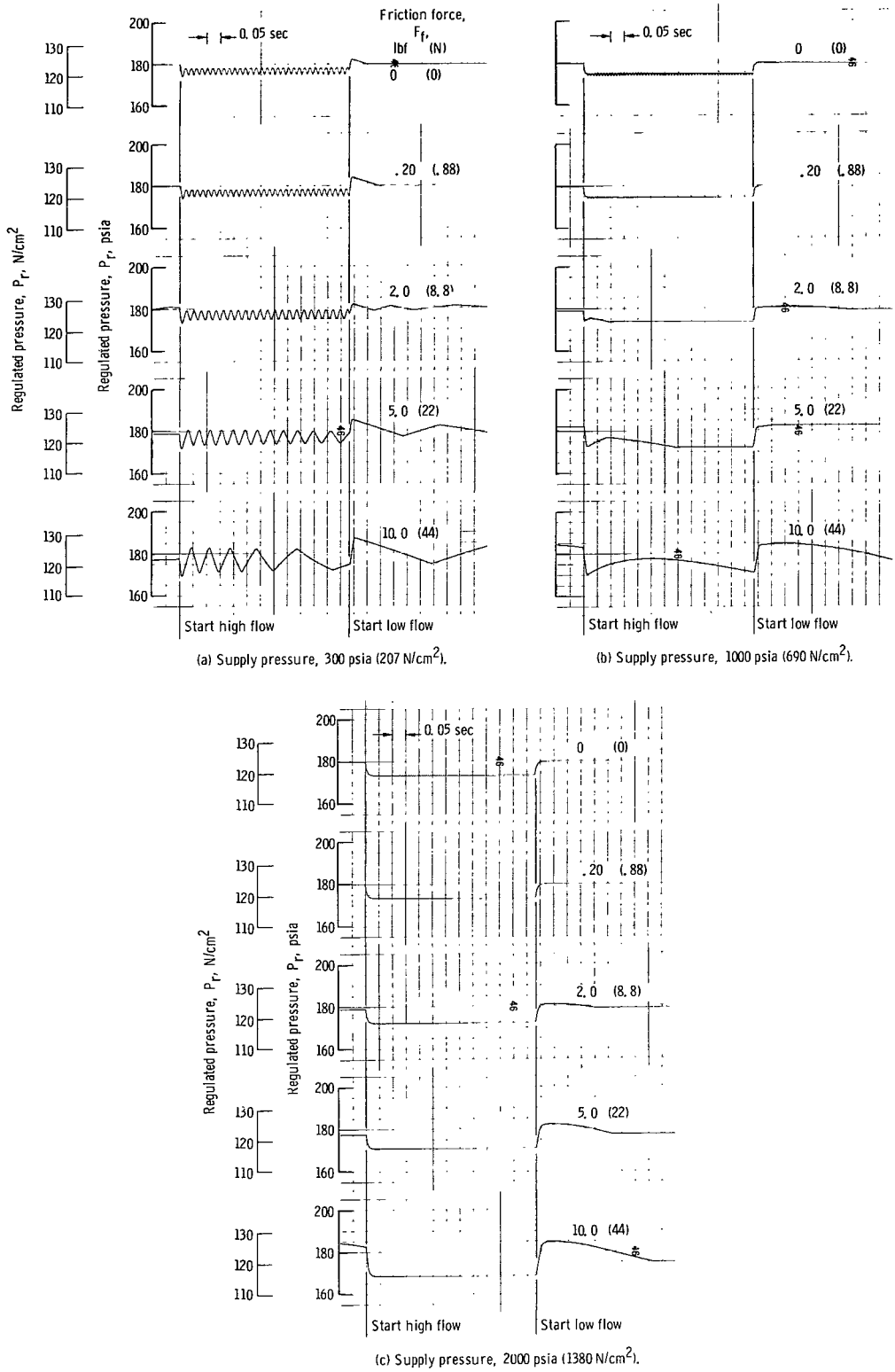

(a) Supply pressure, 300 psia (207 N/cm^2).

(b) Supply pressure, 1000 psia (690 N/cm^2).

(c) Supply pressure, 2000 psia (1380 N/cm^2).

Figure 11. - Simulated regulator response to step changes in output flow orifice area for various values of stem friction. Case II, orifice in series with poppet; spring rate, 100 pounds force per inch (175 N/cm); sensing orifice diameter, 0.125 inch (0.318 cm); output volume, 122 cubic inch (2000 cm^3).

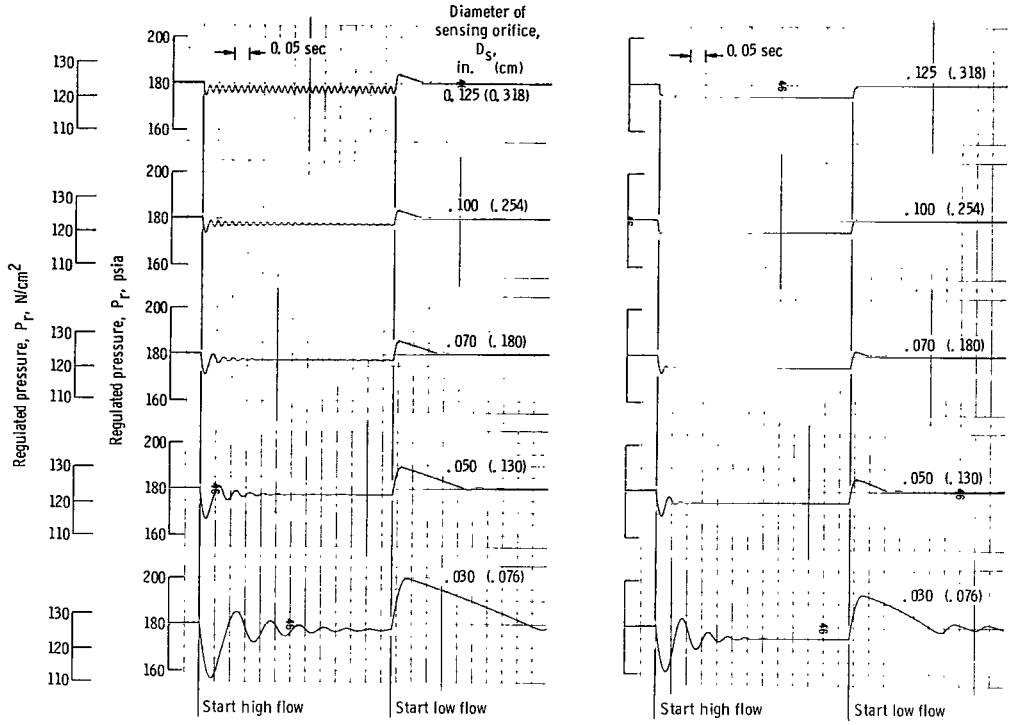

(a) Supply pressure, 300 psia (207 N/cm^2).

(b) Supply pressure, 1000 psia (690 N/cm^2).

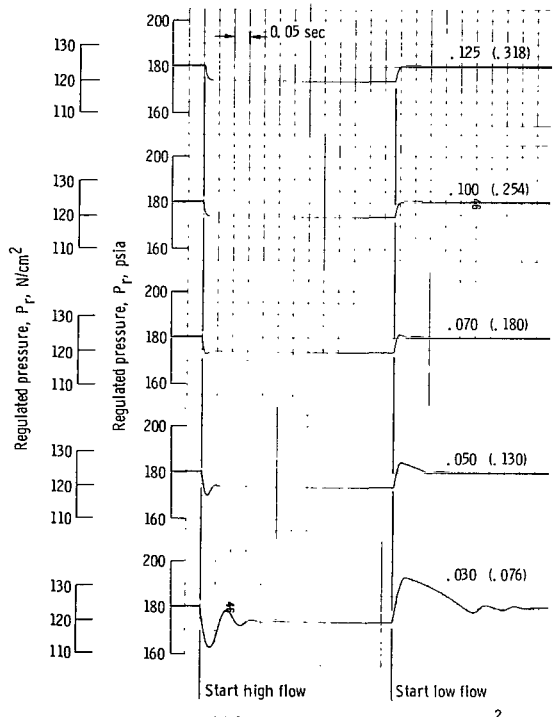

(c) Supply pressure, 2000 psia (1380 N/cm^2).

Figure 12. - Simulated regulator response to step changes in output flow orifice area for various sensing orifice diameters. Case II - orifice in series with poppet; spring rate, 100 pounds force per inch (175 N/cm); stem friction, 0.20 pound force (0.88 N); output volume, 122 cubic inches (2000 cm^3).

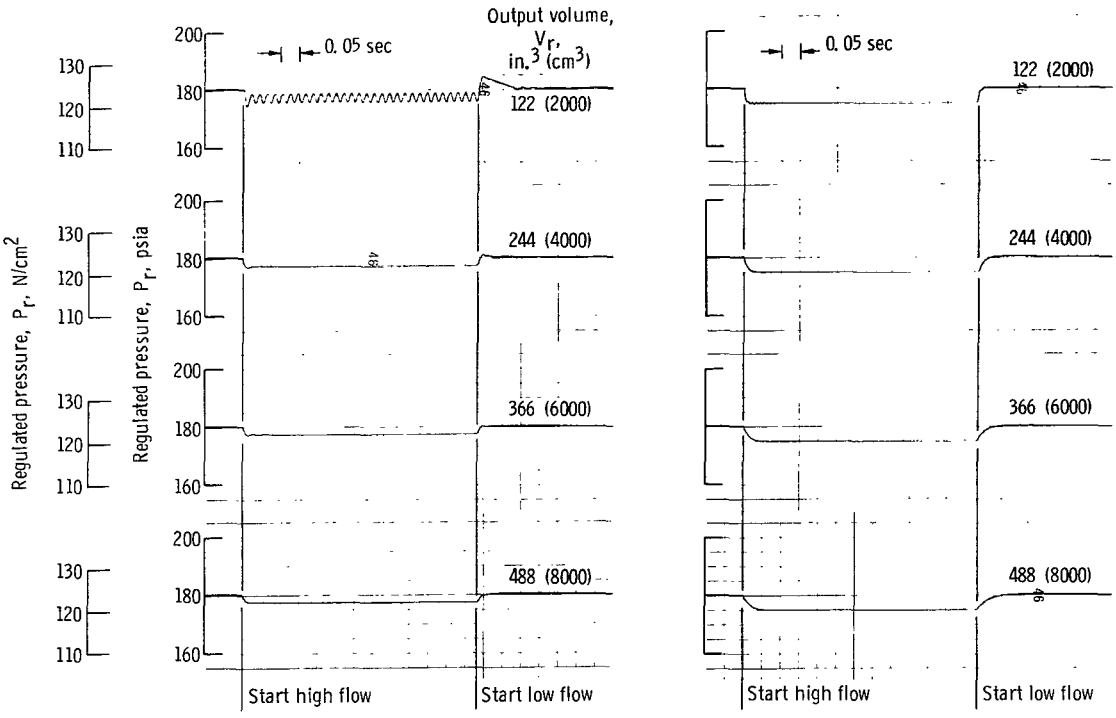

(a) Supply pressure, 300 psia (207 N/cm^2).

(b) Supply pressure, 1000 psia (690 N/cm^2).

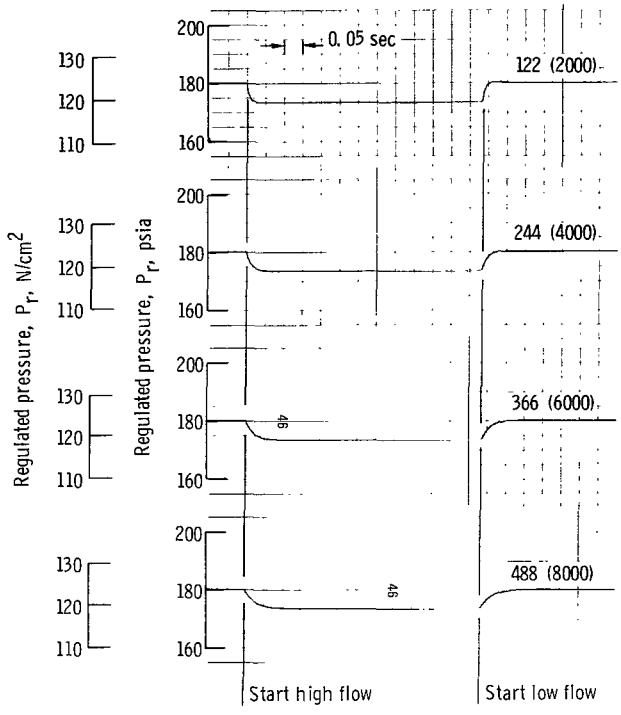

(c) Supply pressure, 2000 psia (1380 N/cm^2).

Figure 13. - Simulated regulator response to step changes in output flow orifice area for various values of output volume. Case II, orifice in series with poppet; spring rate, 100 pounds force per inch (175 N/cm); stem friction, 0.20 pound force (0.88 N); sensing orifice diameter, 0.125 inch (0.318 cm).

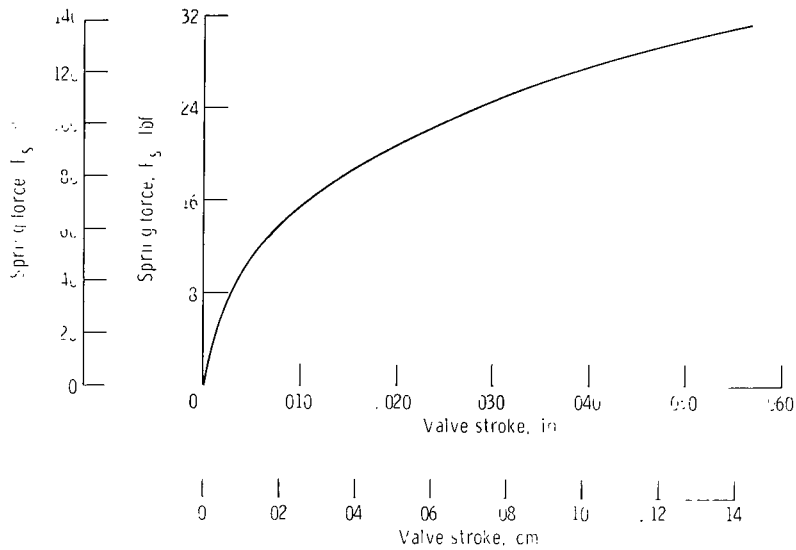

Figure 14 - Spring characteristics used in Case III, Brayton cycle regulator

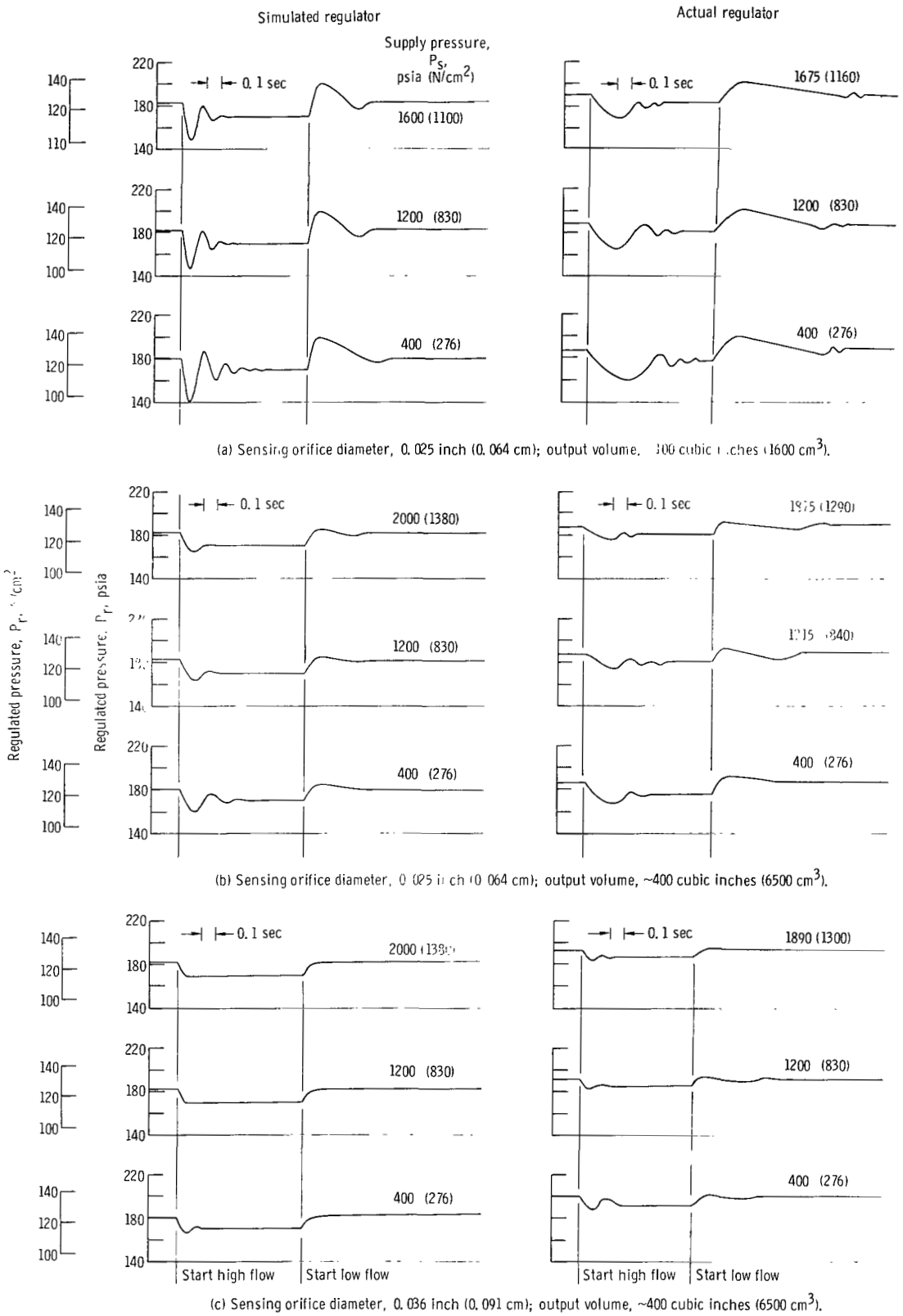

(a) Sensing orifice diameter, 0.025 inch (0.064 cm); output volume, 100 cubic inches (1600 cm^3).

(b) Sensing orifice diameter, 0.025 inch (0.064 cm); output volume, ~400 cubic inches (6500 cm^3).

(c) Sensing orifice diameter, 0.036 inch (0.091 cm); output volume, ~400 cubic inches (6500 cm^3).

Figure 15. - Comparison of actual Brayton cycle regulator's response to step changes in output flow orifice area with response of the Case III simulation of the Brayton cycle regulator. Friction force, 0.20 pound force (0.88 N).

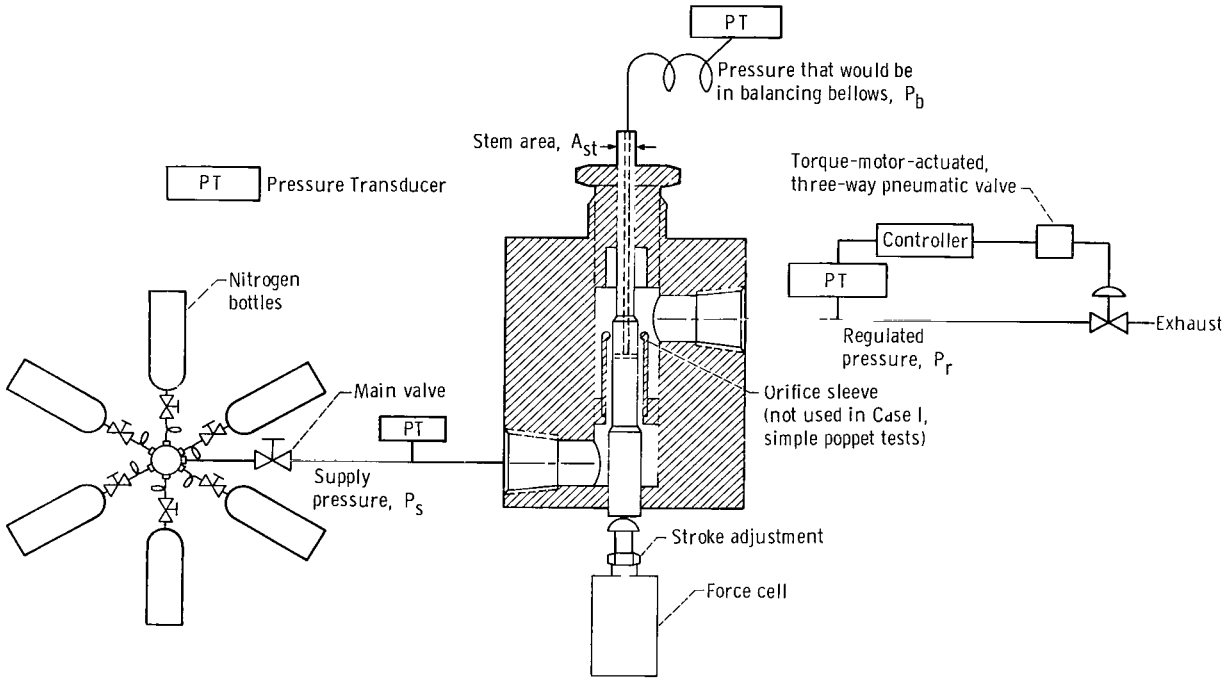

Figure 16. - Test setup for measuring flow forces on poppet-type valve.

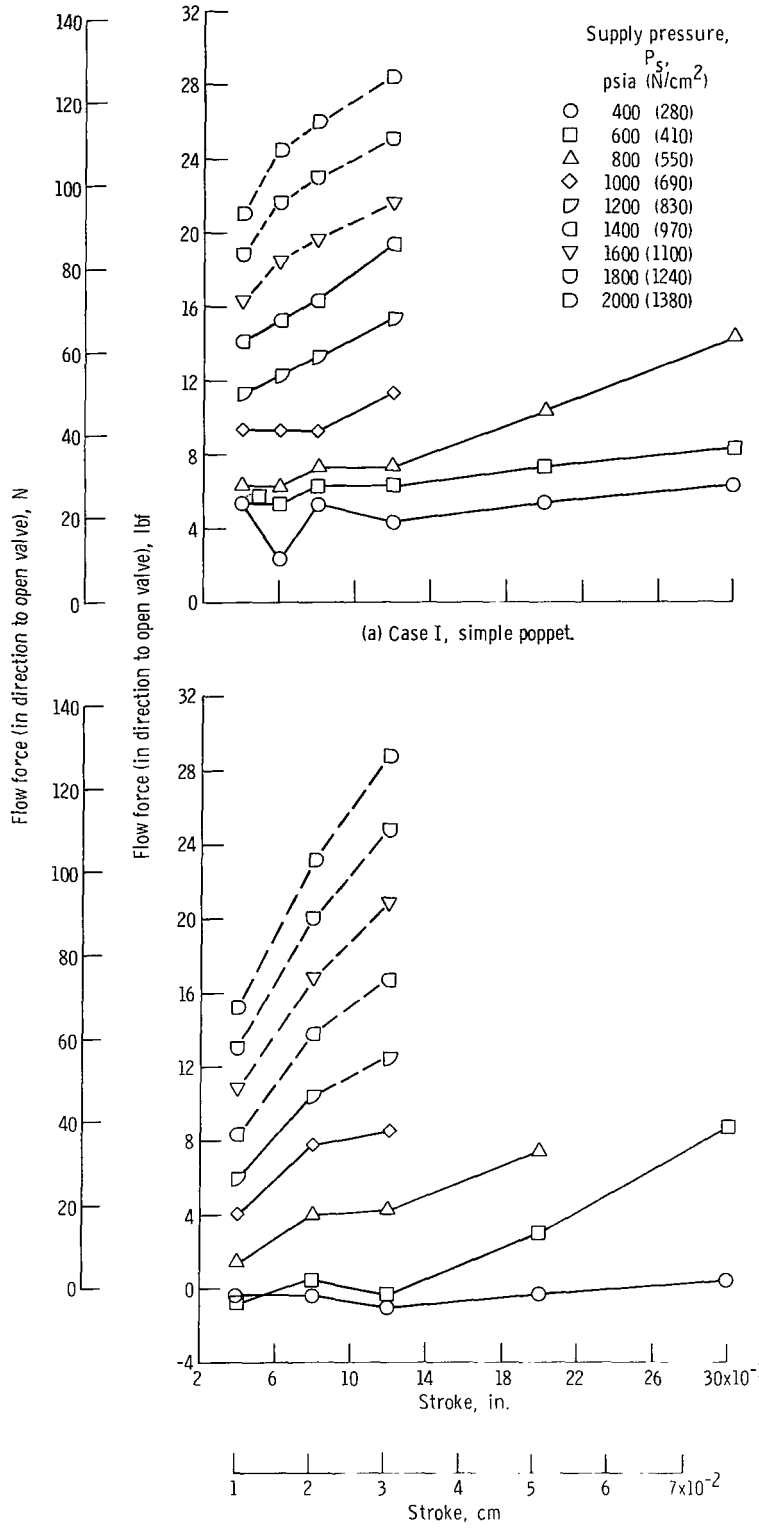

(a) Case I, simple poppet.

(b) Case II, orifice in series with poppet.

Figure 17. - Experimentally determined flow forces as function of stroke

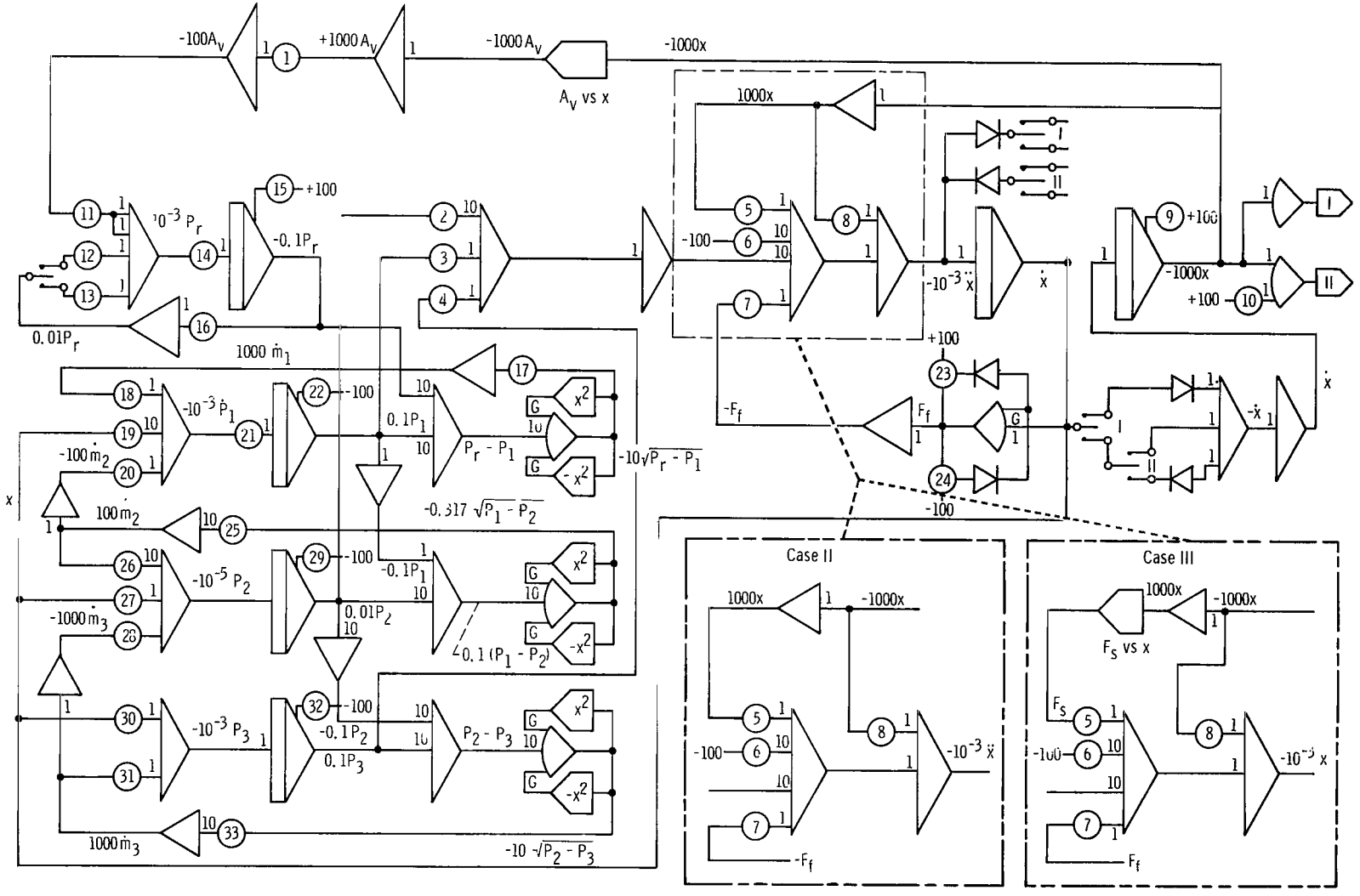

Figure 18. - Analog computer circuit. Main circuit shown is circuit for simple poppet, Case 1. Changes to circuit required for Case II and Case III are shown in insets. Potentiometer settings are listed in table II. Time scale, 1000.

"The aeronautical and space activities of the United States shall be conducted so as to contribute . . . to the expansion of human knowledge of phenomena in the atmosphere and space. The Administration shall provide for the widest practicable and appropriate dissemination of information concerning its activities and the results thereof."

—NATIONAL AERONAUTICS AND SPACE ACT OF 1958

NASA SCIENTIFIC AND TECHNICAL PUBLICATIONS

TECHNICAL REPORTS: Scientific and technical information considered important, complete, and a lasting contribution to existing knowledge.

TECHNICAL NOTES: Information less broad in scope but nevertheless of importance as a contribution to existing knowledge.

TECHNICAL MEMORANDUMS: Information receiving limited distribution because of preliminary data, security classification, or other reasons.

CONTRACTOR REPORTS: Scientific and technical information generated under a NASA contract or grant and considered an important contribution to existing knowledge.

TECHNICAL TRANSLATIONS: Information published in a foreign language considered to merit NASA distribution in English.

SPECIAL PUBLICATIONS: Information derived from or of value to NASA activities. Publications include conference proceedings, monographs, data compilations, handbooks, sourcebooks, and special bibliographies.

TECHNOLOGY UTILIZATION PUBLICATIONS: Information on technology used by NASA that may be of particular interest in commercial and other non-aerospace applications. Publications include Tech Briefs, Technology Utilization Reports and Technology Surveys.

Details on the availability of these publications may be obtained from:

SCIENTIFIC AND TECHNICAL INFORMATION OFFICE

NATIONAL AERONAUTICS AND SPACE ADMINISTRATION

Washington, D.C. 20546